

A Modified Algorithm based on The Equal-Areas PWM for The Extend of Linear Operation of A Microprocessor-Controlled PWM-VSI

F. Paterakis[†], D. Nafpaktitis[†], M. Darwish[‡], G. Koulouras[†]

[†]Department of Electronic Engineering, Technological Educational Institute of Athens, Greece

[‡] School of Engineering and Design, Brunel University, London, UK

Abstract— A modified algorithm based on the Equal-Areas PWM (EAPWM) is being presented in order to extend the linear operation of the inverter in the over-modulation region, while improving the voltage output in terms of fundamental harmonic component amplitude and Total Harmonic Distortion (THD). EAPWM provides an alternative to Regular Sampling (RS) PWM and Space Vector PWM (SVPWM) strategies. EAPWM is a direct digital PWM method that uses the equal areas theorem to determine the pulse widths. This method maintains the commutations through a complete fundamental cycle, in contrast to naturally and regular sampling PWM techniques, where switched pulses progressively disappear for values of modulation index M greater than unity. In addition, this algorithm reveals several linear operating regions of controlling the output fundamental. Simulation and experimental work carried out using a single-phase voltage source inverter (VSI), showing less harmonic content is present for the first harmonic cluster at the switching frequency, compared to (RS) PWM and Space Vector PWM (SVPWM) strategies. This method is suitable for robotic applications where online control through a microcontroller is needed to drive rotating type loads such as ac motor drives and stepper motors.

Keywords— Equal Areas PWM, modulation index, overmodulation, THD, direct PWM, motor drive

Copyright©2017. Published by UNSYSdigital. All rights reserved.
DOI: <https://doi.org/10.21535/ijrm.v5i1.983>

I. INTRODUCTION

IN recent years, voltage source inverters (VSI) have been widely utilized to adjustable speed AC drives, uninterrupted power supplies (UPS), renewable energy systems, robotic applications, electric vehicles, frequency depended systems, etc. The quality of the output of a VSI is significantly depended on the chosen pulse width modulation (PWM) scheme. The primary objective for all PWM schemes is to calculate the converter switching-on times in order to create the desired target output voltage.

The available schemes can be broadly classified as carrier-modulated PWM and programmed PWM schemes [1]. The actual PWM process in carrier modulated PWM methods is

usually a simple comparison between a reference waveform and a saw tooth or a triangular carrier waveform. Then again, the attenuation of wanted fundamental component of the output waveform, the increased switching frequencies and the generation of high frequency harmonic components previously not present, are their main drawbacks [2]. Regular sampling techniques enable the online implementation on digital based systems making these methods widely accepted while programmed PWM techniques such as SVPWM are more difficult to implement due to large computational effort [3].

In a PWM inverter the voltage gain is being determined by the ratio of the output fundamental voltage to the input DC voltage. Regarding the conventional sinus PWM (SPWM) which is the most widely used method in industry, in a three-phase PWM inverter this ratio is limited to 0.87 otherwise output fundamental is 87% of the input DC voltage. To overcome this drawback of poor use of the input DC source significant research work has been undertaken revealing different concepts and performance [4]-[13].

Since, Buja and Indri *et al.* [4] and King *et al.* [5] proposed their modification of the shape of the usual modulating wave used in the PWM sub-oscillation technique, to increase the maximum peak value of the output voltage fundamental component, it has been gradually recognized that maximum modulation index of a three-phase PWM based inverter can be increased by injecting a common mode third-harmonic component into the modulating waveform. King introduced the concept of applying triplen harmonics to produce flat-topped phase waveforms to improve the efficiency of a Class B transistor inverter [5]. Since, King did not identify the amount of each triplen harmonic to be introduced, Houldsworth and Grant determined the optimum amplitude of the third harmonic, to one-sixth that of the fundamental, for the maximum increase of the voltage output [6]. Arguing, that an increased amount of triplen harmonics could result to reduced harmonic distortion researchers Bowes and Midoun *et al.* [7] and Boys and Walton *et al.*[8] proposed that the optimum third-harmonic injection component should have an increased magnitude of 25% of the target fundamental. Hava and Lipo, *et al.* [9] presented an analytical study of the carrier-based PWM techniques used for

Corresponding author: Fotis Konstantinos Paterakis
(e-mail: fpateras@gmail.com)

This paper was submitted on Oct 23, 2017; and accepted on Oct 23, 2017.

the over-modulation region, showing that discontinuous PWM (DPWM) techniques are preferred for high modulation indices where SVPWM is better suited for low indices. The concept of third-harmonic injection was also used by Tamaly and Enjeti to reduce harmonics in the utility interface of wind, photovoltaic and fuel cells power systems by circulating third-harmonic current injection to reduce utility line current harmonics in an SCR converter [10]. Optimal regular-sampled techniques for three-phase inverters are presented by Bowes and Holliday *et al.* [11], highlighting and comparing the characteristics, performance, and implementation of each PWM technique. Eltamaly *et al.* [12] using the effective technique of circulation of third harmonic current from dc-link to the line currents, introduced a single-phase controlled converter in the injection path to control the angle of injection current for each firing angle of three-phase controlled converter. Ramanan *et al.* [13], proposed an alternative PWM method which introduced a modified reference as well as a modified carrier to be used for generating the PWM pattern, while claiming that the proposed PWM technique enhances the fundamental by 19.35% with regard to the conventional Sinusoidal PWM (SPWM). Shayestehfard, Mekhilef and Mokhlis proposed a scalar method that directly uses line-to-line voltages as reference signals, in order to achieve the maximum possible output voltage without injecting a zero-sequence signal [14]. A comprehensive analysis of the digital implementation of the asymmetric right align unipolar regular sampling (RS) PWM and SVPWM techniques along with the proposed left align (LA) SVPWM technique has been carried out by Trigg and Dehbonei on [15]-[16].

This paper proposes an alternative solution to extend the linear operation of the inverter, by modifying the algebraic algorithm of EAPWM that was first introduced in [17]-[18]. A review of the basic EAPWM algorithm is firstly presented, followed by the algorithm modifications. The proposed modified algorithm is capable of penetrating to the over-modulation region in a linear manner by retaining the commutations in the over-modulation region, while increasing the gain of the fundamental component. Instead of introducing triplen harmonics to gain the ability to increase the modulation index or creating discontinuity in the sinus reference waveform, it resets the modulation index only for the over-modulated region, to an optimum value of M in order to recalculate the pulse widths and retain the commutations while avoiding any overlaps. In addition, low order harmonics that are introduced by the over-modulation process, present significantly lower amplitude by the fact that, overlapped pulses are recalculated using the optimum value of the modulation index instead of a pulse dropping in the over-modulated area. The overall harmonic performance is improved.

II. REVIEW OF THE BASIC THEORY OF EAPWM

The equal-areas PWM can be described as: switching so that the integrated area of the target reference waveform over the carrier interval, is the same as the integrated area of the converter switched output. Using Figure 1 and assuming that the half sinusoidal signal can be split in five equal intervals

(with duration d), pulse's active time t_{pJ} (i.e. t_{p2} for the 2nd interval J) can be calculated, assuming that the area of the pulse (defined by ABCD points) must be equal with the area defined by EFGH points.

$$E_{ABCD} = E_{EFGH}$$

Thus, using the integrals of the areas this equality can be expressed as:

$$\omega t_{p2} U_{pulse} = \int_{\omega d}^{2\omega d} U_{sin} \sin(\omega t) d\omega t \quad (1)$$

By solving (1), pulse width duration is derived by (2) and pulse's firing time by (3):

$$t_{pJ} = \frac{U_{sin}}{\omega \cdot U_{pulse}} \left\{ \cos[(J-1)\omega d] - \cos(J\omega d) \right\} \quad (2)$$

$$t_{\epsilon J} = (J-1)d + \frac{1}{2}(d - t_{pJ}) \quad (3)$$

where, modulation index M is defined as:

$$M = \frac{U_{sin}}{U_{pulse}} \quad (4)$$

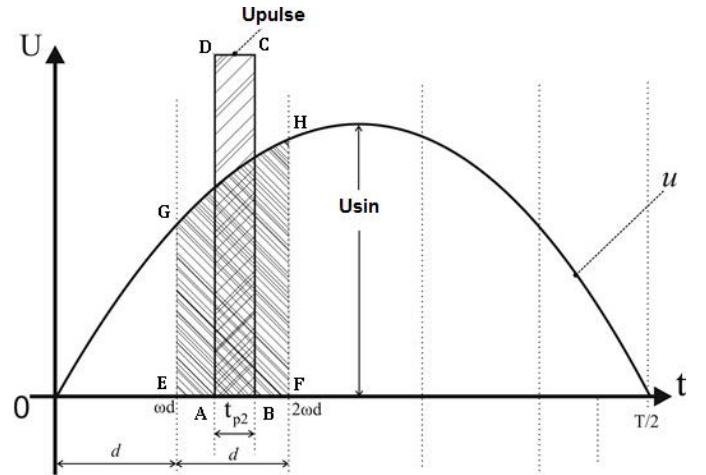


Figure 1 Illustration of the EAPWM

The firing and closing time t_k of a random J pulse in respect to its duration t_{pJ} and firing time $t_{\epsilon J}$ is given by:

$$t_k = t_{\epsilon J} + \left(\frac{1 + (-1)^k}{2} \right) \cdot t_{pJ} \quad (5)$$

$$J = \frac{1 + 2k + (-1)^{k+1}}{4} \quad (6)$$

where k is an indicator showing the rising and falling of every pulse. In this case for five pulses, $J = 1 \dots 5$ and

$k = 1 \dots 10$. So, t_1 is the firing time of first pulse, t_2 is the closing time of first pulse, t_3 is the firing time of second pulse, etc. All times are calculated until $\pi/2$.

The Fourier expansion of the unipolar waveform when n is an odd integer, is described by:

$$u(t) = \sum_{n=1,3,5,\dots}^{\infty} b_n \sin(n\omega t) \quad (7)$$

$$b_n = -\frac{4U_{dc}}{n\pi} \sum_{k=1}^{k=A_p} (-1)^k \cos(n\omega t_k) \quad (8)$$

As in naturally and regular sampled SPWM techniques, the modulation index M cannot be set higher than unity because overlaps between the pulses will occur. For odd number of pulses (A_p), first overlap is occurring on the centered-middle pulse. However, an optimum-marginal value of the modulation index can be calculated avoiding any overlaps. In [Figure 2](#), the limit that modulation index can reach is illustrated.

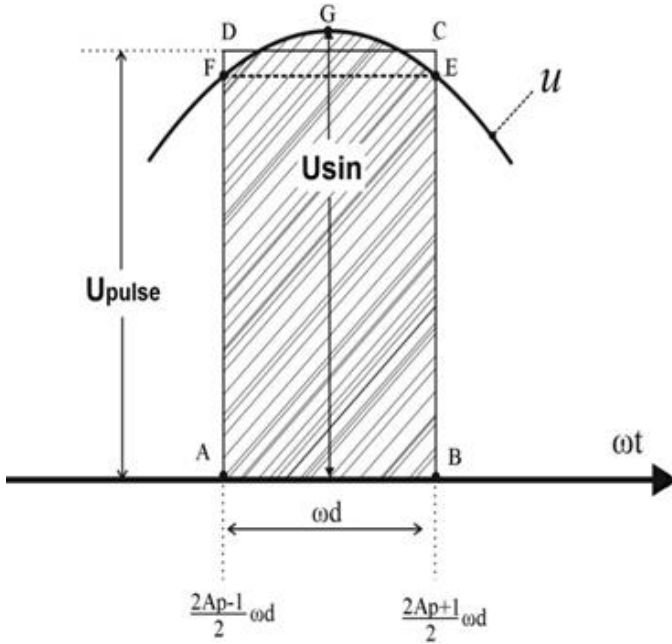


Figure 2 Derivation of the marginal modulation index M

The decrease of the U_{pulse} value implies a corresponding increase at the duration of the pulse. The necessity here is to decrease the U_{pulse} in such a level where the corresponding duration of the pulse t_p , will be less or equal to time interval ωd . Then, as shown in [Figure 2](#), the U_{pulse} will exist between U_{sin} and \overline{FE} . The minimum U_{pulse} can be calculated using the equality that, the area ABCD must be equal with the hatched area ABEGF. This equality can be expressed as:

$$\omega d \cdot U_{pulse} = \int_{\frac{A_p-1}{2}\omega d}^{\frac{A_p+1}{2}\omega d} U_{sin} \sin(\omega t) d\omega t \quad (9)$$

So, the marginal U_{pulse} concludes to:

$$U_{pulse-m} = U_{sin} \frac{2A_p}{\pi} \sin\left(\frac{\pi}{2A_p}\right) \quad (10)$$

And the new optimum-marginal modulation index is now using the new $U_{pulse-m}$.

$$M_m = \frac{U_{sin}}{U_{pulse-m}} \quad (11)$$

The simulation results for the voltage output and the harmonic spectra for the case of five pulses ($A_p = 5$ and frequency ratio $m_f = 5$) is illustrated on [Figure 3](#) and [Figure 4](#), respectively. The modulation index M used for the simulation is the optimal-marginal where is extended to $M_m = 0.9837$, while the $THD = 53.13\%$ is calculated until the 50th harmonic.

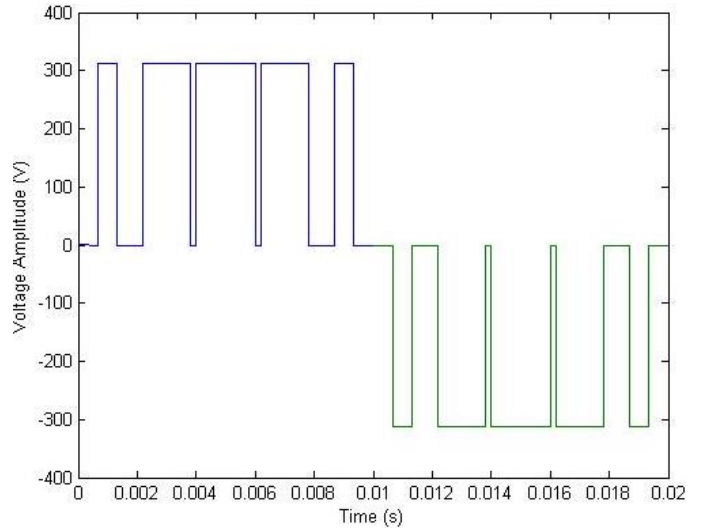


Figure 3 Voltage output for $m_f=5$. The modulation index is $M=0.9837$ and the voltage amplitude of the fundamental is $U(1)=217.29$ V

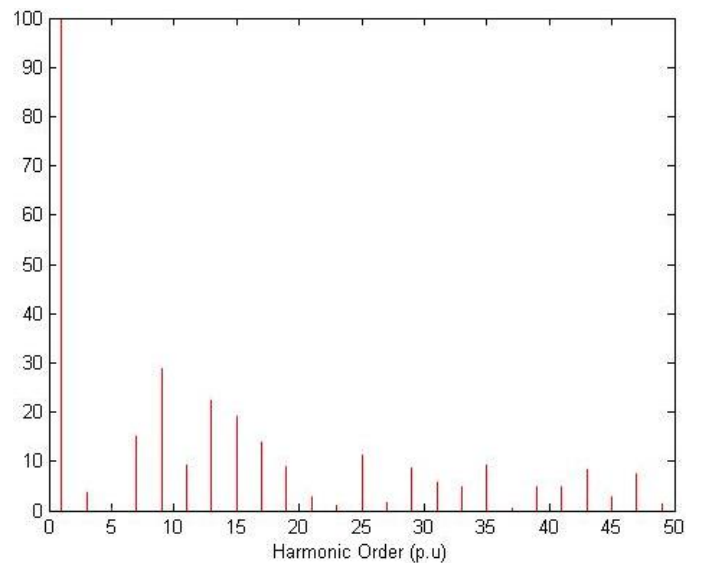


Figure 4 The harmonic spectra for $M = 1.0166$ and $m_f = 5$

Worth noting, that on the conventional unipolar SPWM each phase leg is switching at a frequency derived from the carrier signal. In this case, since a carrier signal is not present, the switching frequency and thus the frequency modulation ratio m_f is set thru the number of pulses A_p on a half-period. Each phase leg will be then switched at half the overall switching frequency (f_s) since the pwm pulses will be produced only for the half-period of the fundamental signal. Since, the number of pulses A_p will always be an odd integer, the frequency modulation ratio m_f will be an odd integer as well (i.e. if $A_p = 11$, $f_s = 1.1$ kHz, for phase-leg A $f_{sA} = 550$ Hz so $m_f = f_{sA}/f_o = 11$, where $f_o = 50$ Hz is the fundamental frequency).

III. MODIFIED ALGORITHM

The basic principle of the proposed algorithm in order to gain the ability to increase the fundamental component and extend the inverters' linear region of operation is a modification in the modulating reference waveform (Figure 5).

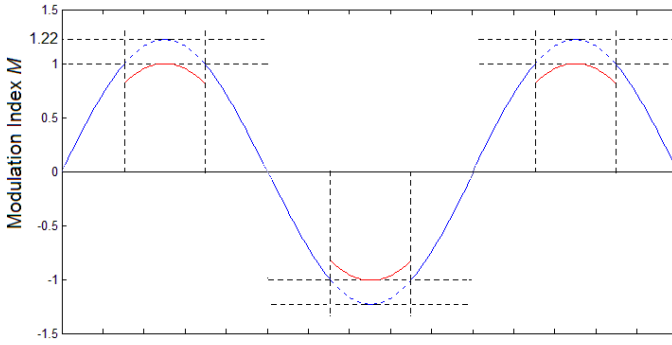


Figure 5 Modified modulating waveform

Instead of creating discontinuity in the reference waveform or reducing the peak magnitude of the sinus reference waveform and injecting a certain amount of triplen-harmonics, the algorithm calculates and uses the optimum value of the modulation index M_m at the given switching frequency in order to recalculate the pulse widths of the overlapped pulses hence retaining the commutations. A case of five pulses per half period will be used to demonstrate how the algorithm works.

As the number of pulses is set to $A_p = 5$ then five intervals will be created in a half-period of the fundamental frequency, meaning that if $f_o = 50$ Hz the period is $T = 20$ ms. Then, five equal time intervals ωd have a duration of $(10 \text{ ms})/5 = 2$ ms (Figure 1). If the initial modulation index is set to $M = 1.5$, the program will start to calculate the pulse widths from left to right until $\pi/2$, using $M = 1.5$. As it calculates the widths of the pulses it calculates as well the starts and endings of each pulse (t_k). After each calculation, the algorithm checks if the pulse's duration time, overlapped the time interval ωd . Now, if an overlap occurs then it recalculates the duration time of the corresponding pulse but now using the optimum-marginal modulation index M_m from equation (11) (which is always close to unity) to prevent overlaps between pulses. That means that the early pulses are calculated with the initial $M = 1.5$ and the latter pulses (closer to the center), that have exceed the time interval, with the optimum-marginal M_m from equation (11).

The optimum-marginal M_m needs to be calculated only once, since it depends only by the number of pulses A_p .

In the case of M exceeds unity ($M > 1$) the overlaps occur firstly at the center of the sinus waveform and gradually spread to the entire PWM waveform. The number of the overlapped pulses, that need to be recalculated for a fixed switching frequency, depends on the initial modulation index M . As M increases more overlaps occur, thus the greater the range that the optimum modulation index (M_m)-waveform is to occupy, into the final modulating waveform. When this change on modulation index M is made, the inverter enters a new linear region of operation, increasing the amplitude of the fundamental component until new overlaps again occur and reset of the modulation index is again needed. This procedure can be observed in Figure 6 where the variation of the fundamental component as a function of the modulation index is graphed. Every change on the slope of the graph indicates a wider clamping to the M_m waveform. The system converges to unity as the modulation index increases since the initial reference waveform is being replaced by the optimum-marginal waveform of $M_m \approx 1$.

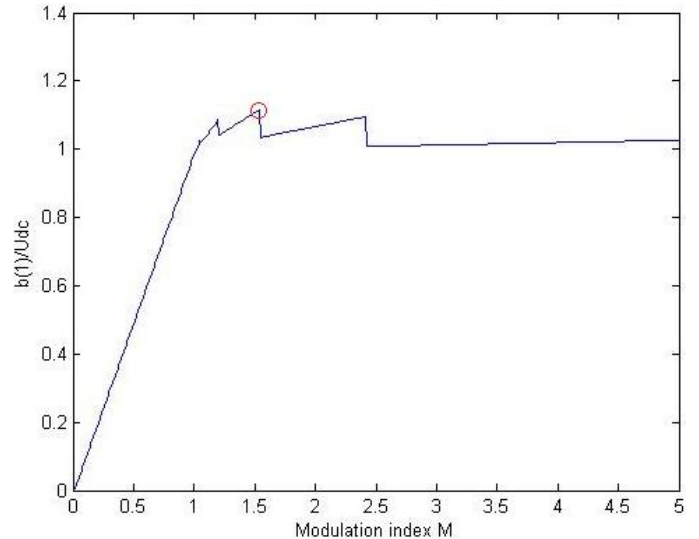


Figure 6 Fundamental component vs. Modulation index. Linear regions of operation after each recalculation for $m_f = 11$

Using Figure 6, the maximum gain of modulation for the specific switching frequency, can be easily identified (every peak). In the case of $m_f = 11$, $f_s = 1.1$ kHz, the higher gain is reached at $M = 1.53$ where the gain of the fundamental amplitude is at 11.5%. As illustrated in Figure 5, the modified modulating waveform is reconstructed by replacing the over-modulation range of the initial modulation depth $M = 1.22$, to clamp to the optimum-marginal modulation index $M_m \approx 1$ – maintaining in a way, a sinus PWM. It is well known that the optimum harmonic components, along with the maximum fundamental amplitude occur when a modulating index of unity depth is applied. Consequently, as the over-modulating range of the initial modulating waveform ($M > 1$) is being replaced by the optimum modulation index ($M_m \approx 1$), the overall harmonic spectrum is expected to be improved in terms of

THD. That explains the superior harmonic performance in terms of THD and low order harmonics compared to RS PWM, and SVPWM.

This algorithm gives the advantage of increasing the fundamental component without pulse dropping as in (RS) PWM in the over-modulation region. In addition, the linear operation can be extended without the stage of injecting certain amounts of triplen harmonics or creating discontinuity to the reference waveform. In [Figure 7](#) and [Figure 8](#), where the harmonics spectrum is plotted for the cases of $m_f = 5$ and $m_f = 11$ with $M = 1.5$, the fundamental harmonic component shows an increment by a factor of 6.4 % and 6.7 % respectively. Low order harmonics are present but with reduced amplitude. For the case of [Figure 7](#) where $m_f = 11$, third harmonic component participates only by a factor of 6.5 % of the fundamental and the fifth harmonic component only by 2.45 %.

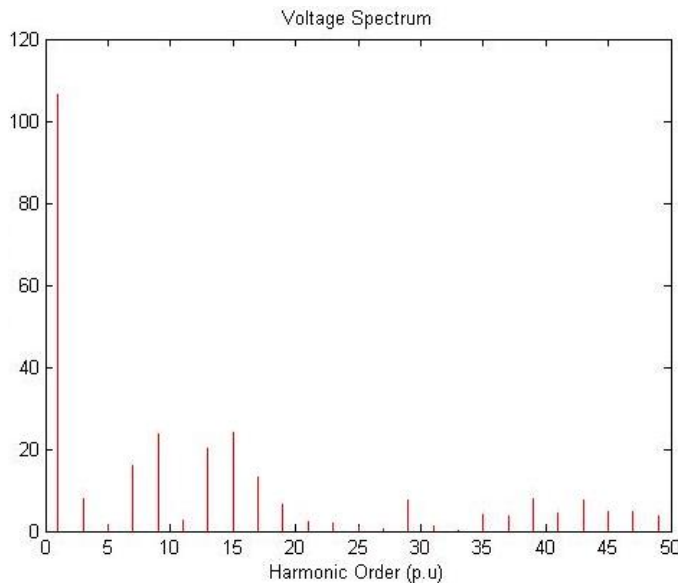


Figure 7 The FFT of the modified algorithm for $m_f=5$

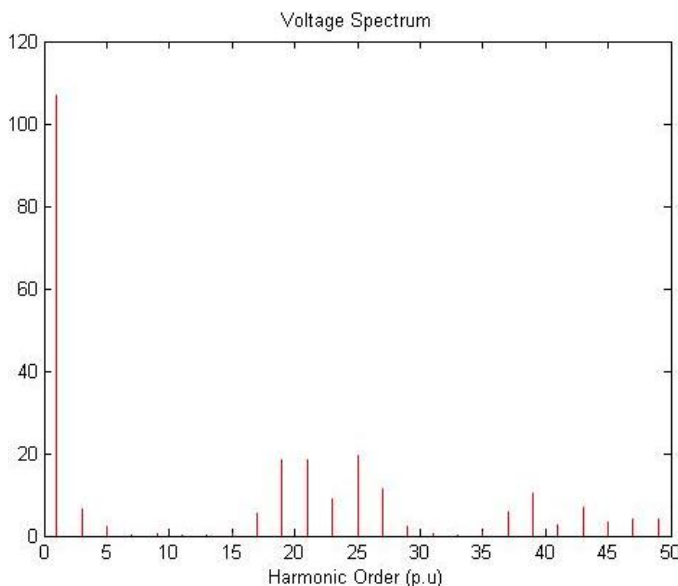
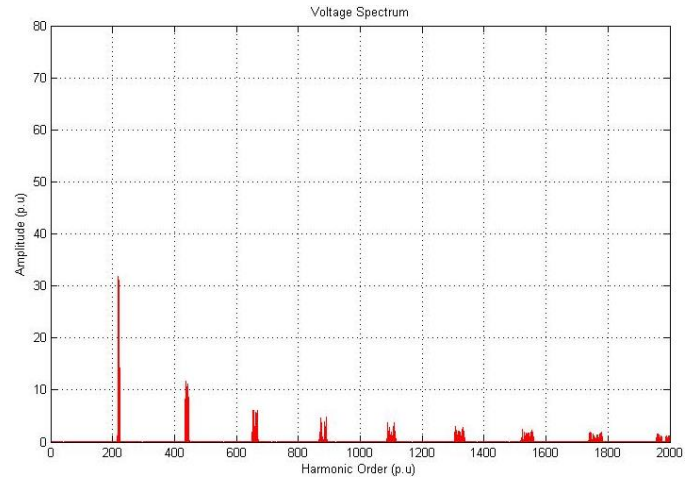


Figure 8 The FFT of the modified algorithm for $m_f=11$

IV. COMPARISON WITH OTHER PWM METHODS

The research of Trigg and Dehbonei [\[14\]-\[15\]](#) is used to compare the results obtained by the EAPWM. To meet the same conditions as possible for the simulation, a modulation index of $M = 0.8$ and switching frequency of $f_s = 11 \text{ kHz}$ is chosen. Frequency domain plots are generated until 100 kHz (2000th harmonic). In [Figure 9](#) the frequency domain is plotted for EAPWM.



50 ohm, and then retested using an inductive load of $L = 25$ mH, $C = 10\mu F$ and $R = 50$ ohm. In [Figure 12](#) and [Figure 13](#), the PWM signals are illustrated along with the current waveform for the specific load. In [Figure 10](#) the experimental setup is illustrated. The software program used for programming the AVR through the Arduino Duemilanove module is the Code Vision AVR.

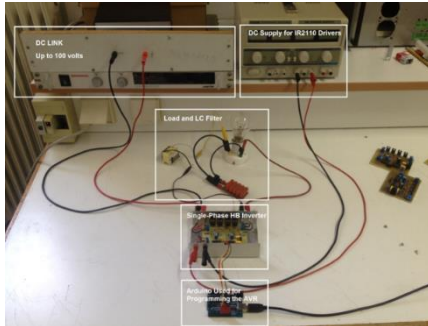


Figure 10 The experimental setup

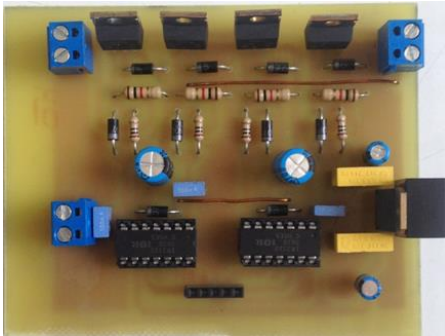


Figure 11

The prototype inverter was built using IRF830 power MOSFETs as the switching devices as shown in [Figure 11](#). This prototype system was configured to have a nominal DC link of 60 volt. Software, MATLAB© and Proteus ISIS were used for simulation purposes.

The experimental results are illustrated based on two modulation indices $M = 1$ and $M = 1.19$ for the switching frequency of $f_s = 1.1$ kHz ($A_p = 11$ in terms of number of pulses). [Figure 12](#) and [Figure 13](#) present the positive half-period PWM signal from the AVR module, the voltage waveform produced using the LC filter, and then the normalized FFT of the output voltage without any filter.

For the case where $M = 1$ and $m_f = 11$ the THD calculated until the 200th harmonic component is at 46.28 % and the rms value of the fundamental component at 42.17 V ([Figure 12](#)). If a modulation ratio of $M = 1.19$ is initially set then the algorithm will recalculate the three middle pulses in order to avoid overlaps and retain commutations. This will result in lower THD at 38.06 % and an rms value of the fundamental component at 46.1 V ([Figure 13](#)). The participation of the low order harmonics, 3rd, 5th and 7th which their presence is avoidable in overmodulation region, is lower than 5 %, showing the advantages of the proposed method.

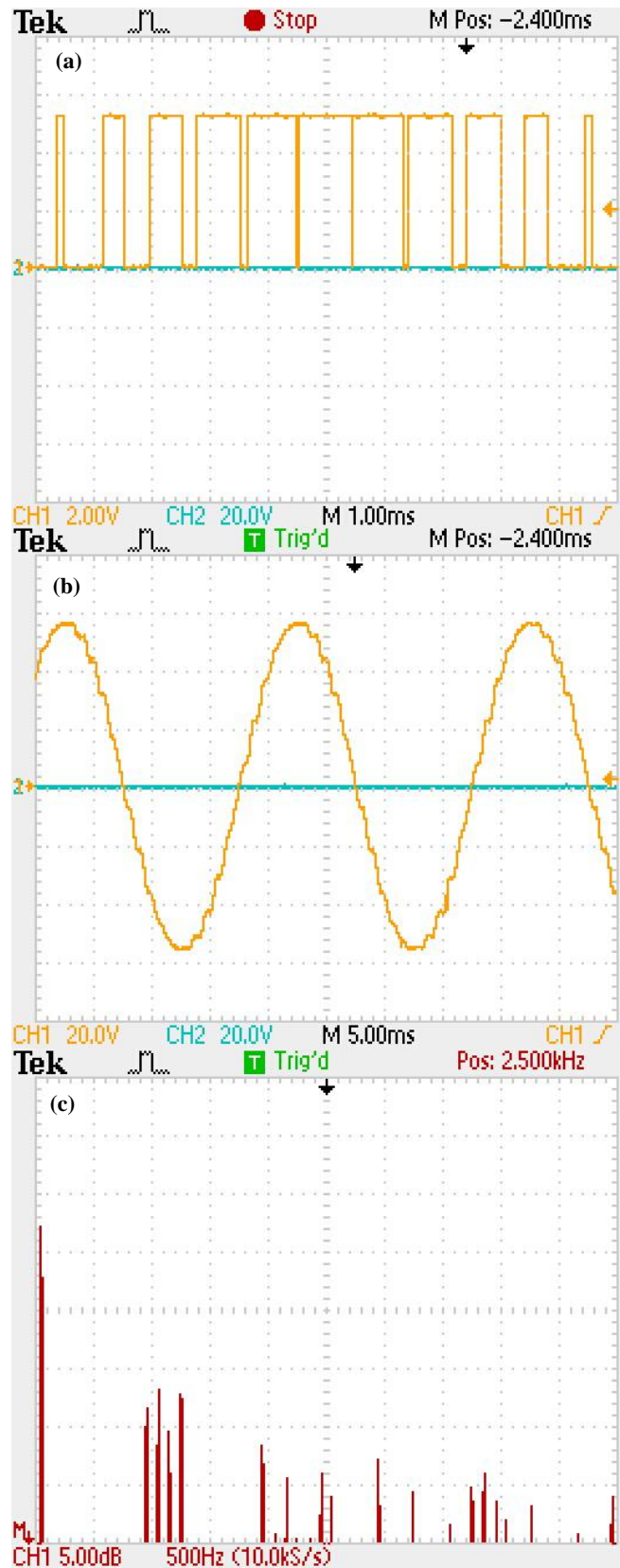


Figure 12 $A_p=11$, $f_s=1.1$ kHz, $m_f=11$, initial $M=1$
 (a) The PWM signal in the positive half-period
 (b) Current waveform for $A_p=11$ with LC filter in the output
 (c) FFT of the single-phase inverter output ($A_p=11$).

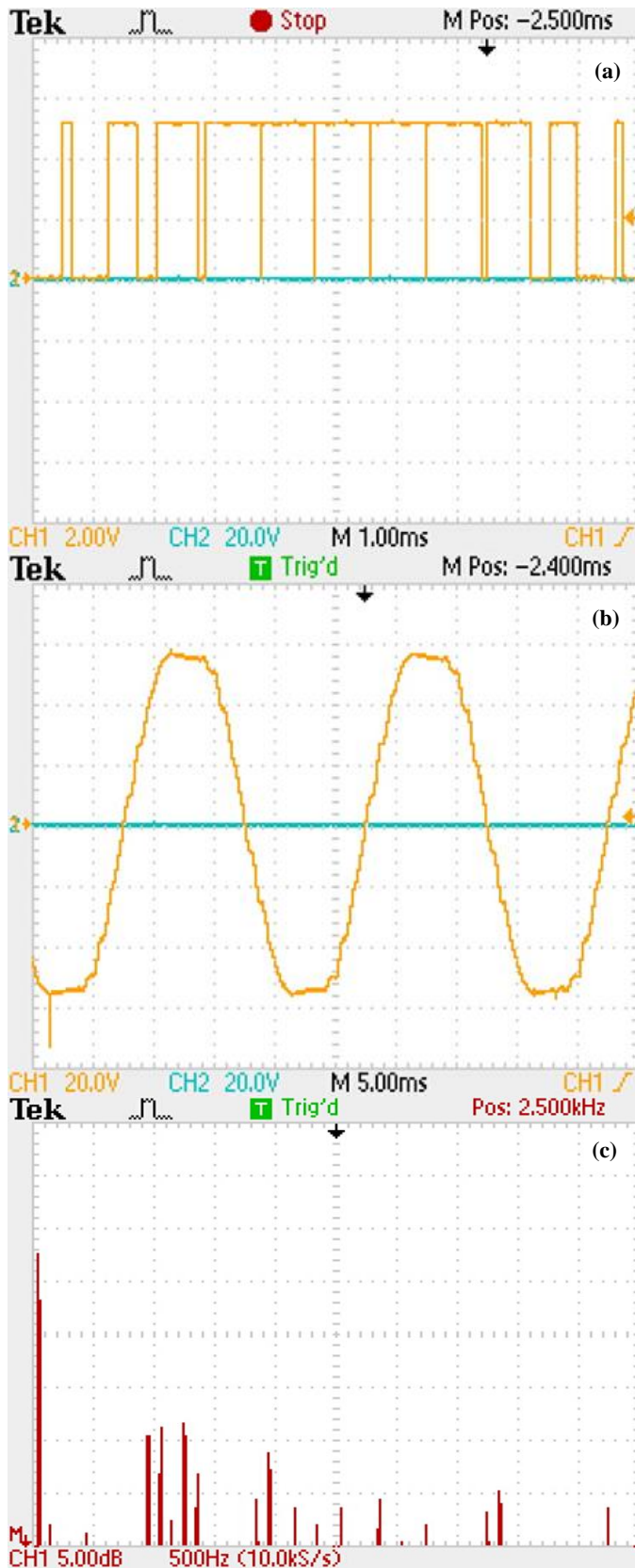


Figure 13 $A_p=11$, $f_s=1.1\text{kHz}$, $m_f=11$, initial $M=1.19$, $k=5$

- (a) The PWM signal in the positive half-period
 (b) Current waveform for $A_p=11$ with LC filter in the output
 (c) FFT of the single-phase inverter output ($A_p=11$).

VI. CONCLUSIONS AND FURTHER WORK

A modified algorithm based on the EAPWM capable of expanding the linear operation of the inverter while penetrating the over-modulation region in a linear manner has been presented. Comparison with RSPWM and SVPWM has been shown the superiority of the proposed method in terms of THD and low order harmonics. In addition, less computational effort is needed since simple algebraic equations are used for the derivation of the pulse width modulation. Experimental results validated the theoretical background. The algorithm is capable of improving the THD as the modulation index exceeds unity depth while creating linear regions of operation through the over-modulation region. This advantage can be very critical in robotic applications when online control of rotating loads such as stepper motor and ac drives is needed. The modified algorithm introduced in this paper will be implemented in a three-phase inverter prototype in order to produce simulation and experimental results for comparison with Third Harmonic Injection techniques and discontinuous PWM methods for three-phase systems. Since EAPWM is a direct-digital PWM modulation, showing improved harmonic response compared to regular sampling SPWM and SVPWM, the modified algorithm will be implemented in a microprocessor-based Multilevel Inverter to investigate the operation of this type of inverter in the over-modulation region. The results of this study can be useful in the development, design and performance evaluation of over-modulation strategies for PWM converters.

REFERENCES

- [1] Holtz, J., "Pulsewidth modulation-a survey," Power Electronics Specialists Conference, 1992. PESC '92 Record., 23rd Annual IEEE, vol., no., pp.11,18 vol.1, 29 Jun-3 Jul 1992.
- [2] Boost, M.A.; Ziogas, P.D., "State-of-the-art carrier PWM techniques: a critical evaluation," Industry applications, IEEE Transactions on, vol.24, no.2, pp.271-280, Mar/Apr 1988.
- [3] Rus, D. C.; Preda, N. S.; Incze, I.I.; Imecs, M.; Szabó, C., "Comparative analysis of PWM techniques: Simulation and DSP implementation," Automation Quality and Testing Robotics (AQTR), 2010 IEEE International Conference on, vol.3, no., pp.1,6, 28-30 May 2010.
- [4] Buja, G. & Indri, G. 1975, "Improvement of pulse width modulation techniques", Archiv f r Elektrotechnik, vol. 57, no. 5, pp. 281-289.
- [5] F. G. King, "A three-phase transistor class-B inverter with sinewave output and high efficiency," in Inst. Elec. Eng. Conf. Publ. 123, Power Electronics, Power Semiconductors and Their Applications, 1974, pp. 204-209.
- [6] John A. Houldsworth, Duncan A. Grant, "The Use of Harmonic Distortion to Increase the Output Voltage of a Three-Phase PWM Inverter", IEEE Transactions on industry applications, Vol. IA-20, No. 5, September/October 1984.
- [7] Halász, S., Bowes, S.R. & Midoun, A. 1985, "Suboptimal switching strategies for microprocessor-controlled PWM inverter drives", IEE Proceedings B Electric Power Applications, vol. 132, no. 6, pp. 344.
- [8] Boys, J.T. & Walton, S.J. 1985, "A loss minimized sinusoidal PWM inverter", IEE Proceedings B Electric Power Applications, vol. 132, no. 5, pp. 260.
- [9] A. M. Hava, R. J. Kerkman and T. A. Lipo, "Carrier-based PWM-VSI overmodulation strategies: analysis, comparison, and design," in IEEE Transactions on Power Electronics, vol. 13, no. 4, pp. 674-689, Jul 1998.
- [10] A. M. El-Tamaly, P. N. Enjeti and H. H. El-Tamaly, "An improved approach to reduce harmonics in the utility interface of wind, photovoltaic and fuel cell power systems," Applied Power Electronics Conference and Exposition, 2000. APEC 2000. Fifteenth Annual IEEE, New Orleans, LA, 2000, pp.1059-1065 vol.2. doi: 10.1109/APEC.2000.822819.

- [11] Bowes, S.R. & Holliday, D. 2007, "Optimal Regular-Sampled PWM Inverter Control Techniques", IEEE Transactions on Industrial Electronics, vol. 54, no. 3, pp. 1547-1559.
- [12] Eltamaly, A.M. 2012, "A novel harmonic reduction technique for controlled converter by third harmonic current injection", Electric Power Systems Research, vol. 91, pp. 104.
- [13] Ramanan, S., Rajaram, K., Ram Kumar, S. & Nagarathinam, B. 2014, "Novel PWM technique for fundamental fortification in voltage source inverters", IEEE, pp. 328.
- [14] Shayestehfard, A., Mekhilef, S. & Mokhlis, H. 2015, "Modified scalar discontinuous pulse-width modulation method for two-level three-wire voltage source inverters under unbalanced and distorted conditions", IET Power Electronics, vol. 8, no. 8, pp. 1339-1348.
- [15] Trigg, M.C., Dehbonei, H. & Nayar, C.V. 2008, "Digital sinusoidal PWMs for a micro-controller based single-phase inverter, Part 1: Principles of digital sinusoidal PWM generation", International Journal of Electronics, vol. 95, no. 8, pp. 819-840.
- [16] Trigg, M.C., Dehbonei, H. & Nayar, C.V. 2008, "Digital sinusoidal PWMs for a micro-controller based single-phase inverter, Part 2: Performance assessment-experimental", International Journal of Electronics, vol. 95, no. 9, pp. 951-972.
- [17] D. Nafpaktitis, G. Hloupis, I. Stavrakas, F. Paterakis., "An Alternative Approach for PWM Modeling in Power Electronics Systems", J. Electrical Systems 7-4 (2011): 438-447.
- [18] D. Nafpaktitis, F. Paterakis, M. Darwish, G. Hloupis., "The Equal Areas Pulse Width Modulation (EAPWM) Method: an alternative approach to programmed PWM schemes", J. Electrical Systems 12-1 (2016): 174-186.